

A FLUTTER MODEL FOR ROTOR BLADES WITH FLAPS

Mark A. Couch*, E. Roberts Wood**

*U.S. Navy/COMSEVENTHFLT, **Naval Postgraduate School

Keywords: *Flutter, Rotor Blades, Flaps, Aeroelasticity,*

Abstract

A three-dimensional, frequency-domain flutter theory for a five Degree-of-Freedom (5DOF) system for rotor blades with trailing-edge flaps is developed. Lagrange's equation using superposition of normal modes and the aerodynamic forces and moments given by two-dimensional strip theory for an incompressible flow is applied to develop a flutter solution. In order to solve the flutter problem, the free vibrations for both the bending and torsional mode shapes and natural frequencies for the rotating blade are determined. To model the flap, the stiffness of the torsional spring for the flap is tuned such that the flap rigid body uncoupled natural frequency can be equated to the flap input frequency, thus allowing analysis of the effect of flap input frequency on the flutter solution.

Three-dimensional aspects are included with sectional variations of mass, geometry and freestream velocity. Aerodynamic effects are examined through different lift deficiency functions. It is assumed that the aerodynamic forces and moments do not change the uncoupled modes shapes. Practical application is demonstrated using a hingeless rotor blade.

1 Introduction

Flutter is normally defined as an aeroelastic, self-excited vibration, in which the external source of energy is the air stream. When flutter occurs, the air stream provides energy to the system more rapidly than it is dissipated by damping [1], [2]. The requirements for designing helicopter rotor

blades to be free of flutter are contained in Federal Aviation Regulations under Aircraft Circular 27-1B for normal category rotorcraft [3] and Aircraft Circular 29-2C for transport category rotorcraft [4]. Section 629 of both circulars state that the rotorcraft must be free from flutter. Additionally, section 629A of AC 29-2C requires "each aerodynamic surface of the rotorcraft must be free from divergence in addition to the requirement of freedom from flutter. The aeroelastic stability evaluations required by this regulation include flutter and divergence. Compliance with this regulatory requirement should be shown by analysis and/or flight test, supported by any other means found necessary by the Administrator. The aeroelastic evaluation of the rotorcraft should include an investigation of the significant elastic, inertia and aerodynamic forces on all aerodynamic surfaces (including rotor blades) and their supporting structure. The forces associated with the rotations and displacements of the plane of the rotors should be considered."

A prevalent design practice of collocating the center of gravity, elastic axis and aerodynamic center has the advantage of decoupling the aerodynamic, elastic and dynamic equations of motion. While this assures freedom from flutter and other aeroelastic phenomena, it provides additional constraints on rotor blade design not normally followed in fixed-wing design. A rotor blade designed with the center of gravity, elastic axis and aerodynamic center coincident at the quarter-chord will be heavier than one free of that restriction. The added weight in the rotor blade may necessitate a larger power plant and a larger gearbox, and the rotor blade itself may be

larger than needed in order to provide the necessary rotor thrust to achieve flight. Also, if strictly followed, this design constraint rules out use of a trailing-edge flap because the aerodynamic center will move when the flap angle is changed [5], [6], and the elastic axis and center of gravity may shift when a trailing-edge flap is incorporated.

Aeroelastic analysis of a rotor blade with a trailing-edge flap is a concern for active vibration control systems such as individual blade control (IBC) and higher harmonic control (HHC) and have been routinely performed using a computational code such as CAMRAD II, CAMRAD/JA, 2GCHAS, UMARC, and others [5], [7], [8]. While these codes are quite capable of predicting rotor vibrations, they all work predominantly in the time domain and require much effort to learn how to use them to the fullest extent of their capabilities. Time history plots are generated and analyzed in order to see if any instability, such as flutter, existed. The lack of a closed-form, frequency-domain solution for the aeroelastic analysis of rotor blades with trailing-edge flaps is very apparent in a review of the literature. Inherent in IBC/HHC analyses is the issue of freeplay and its effect on rotor performance and structural stability [9]. Additionally, Loewy [10] showed how shed layers of vorticity affect Theodorsen's lift deficiency function [11] and influence the unsteady aerodynamic lift and moment equations. While Loewy did not explicitly state that his 2-D theory would apply to rotor blades with trailing-edge flaps, the manner in which the theory was developed allows it to be applied in this manner.

2 Background

2.1 Structural Dynamics

In order to solve the flutter problem, the free vibrations for both the bending and torsional mode shapes and natural frequencies for the rotating blade need to be determined. Typically, the rotor blade is modeled as a series of discrete masses and springs that

approximates the continuous system. For the torsional mode shapes and frequencies, the Holzer method [12] is used, while the Myklestad method [13], [14] is used for the bending, or flexural mode shapes and frequencies. Both methods are effectively step-by-step solutions to either a 2nd order or 4th order differential equation of a lumped-parameter system. The Holzer method written in transfer matrix form is

$$\begin{bmatrix} 1 & 0 \\ -I_{\alpha_n} (\omega_\alpha^2 - \Omega^2 \cos \theta_n) & 1 \end{bmatrix} \begin{bmatrix} \phi \\ T \end{bmatrix}_{n+1} = \begin{bmatrix} 1 & -l_{n,n+1} / [(GJ)_{n+1} + (Ck_a^2)_{n+1}] \\ 0 & 1 \end{bmatrix} \begin{bmatrix} \phi \\ T \end{bmatrix}_n$$

The Myklestad method written in transfer matrix form is

$$\begin{bmatrix} 1 & 0 & 0 & -m_n \omega_h^2 \\ 0 & 1 & 0 & -C_{n+1} \\ 0 & 0 & 1 & 0 \\ 0 & 0 & l_{n,n+1} & 1 \end{bmatrix} \begin{bmatrix} S \\ M \\ \beta \\ z \end{bmatrix}_{n+1} = \begin{bmatrix} 1 & 0 & 0 & 0 \\ l_{n,n+1} & 1 & 0 & -C_{n+1} \\ -\frac{l_{n,n+1}^2}{2(EI)_n} & -\frac{l_{n,n+1}}{(EI)_n} & 1 + \frac{l_{n,n+1}^2 C_{n+1}}{2(EI)_n} & 0 \\ -\frac{l_{n,n+1}^3}{3(EI)_n} & -\frac{l_{n,n+1}^2}{2(EI)_n} & \frac{l_{n,n+1}^3 C_{n+1}}{3(EI)_n} & 1 \end{bmatrix} \begin{bmatrix} S \\ M \\ \beta \\ z \end{bmatrix}_n$$

2.2 Unsteady Aerodynamics

Any general oscillating motion of an aircraft structure can be expressed in terms of translation from and/or rotation about some reference axis, assuming the displacements from equilibrium are small relative to the dimensions of the structure. If that structure contains a portion that is free to rotate about some hinge axis, the general displacement of an element of mass can be expressed in terms of translation from a reference axis, rotation about a reference axis, and rotation about the hinge axis. Assuming the structure under consideration is a helicopter rotor blade that has a trailing-edge flap incorporated at the trailing edge as shown in **Fig. 1**. The reference axis for translation will

be the elastic axis of the undisturbed rotor blade, and the reference axis for blade rotation will also be the elastic axis. Applying thin airfoil theory for the case of an inviscid, incompressible fluid, Smilg and Wasserman [15] showed that the forces and moments per unit span on the airfoil are given as follows:

(1) Wing lift force per unit span:

$$L' = \pi \rho b^3 \omega^2 \left\{ L_h \frac{h}{b} + \left[L_\alpha - \left(\frac{1}{2} + a \right) L_h \right] \alpha + \left[L_\beta - (c-e) L_z \right] \beta \right\}$$

(2) Moment per unit span due to blade rotation about the wing quarter-chord:

$$M' = \pi \rho b^4 \omega^2 \left\{ \left[M_h - \left(\frac{1}{2} + a \right) L_h \right] \frac{h}{b} + \left[M_\alpha - \left(\frac{1}{2} + a \right) (L_\alpha + M_h) + \left(\frac{1}{2} + a \right)^2 L_h \right] \alpha + \left[M_\beta - \left(\frac{1}{2} + a \right) L_\beta - (c-e) \left(M_z - \left(\frac{1}{2} + a \right) L_z \right) \right] \beta \right\}$$

(3) Moment per unit span due to flap rotation about the hinge:

$$T' = \pi \rho b^4 \omega^2 \left\{ \left[T_h - (c-e) P_h \right] \frac{h}{b} + \left[T_\alpha - (c-e) P_\alpha - \left(\frac{1}{2} + a \right) (T_h - (c-e) P_h) \right] \alpha + \left[T_\beta - (c-e) (P_\beta + T_z) + (c-e)^2 P_z \right] \beta \right\}$$

where b is the semi-chord, k is the reduced frequency, the dimensions for a , c and e are shown in **Fig. 1**, and the L , M , T and P terms are listed in Ref [15].

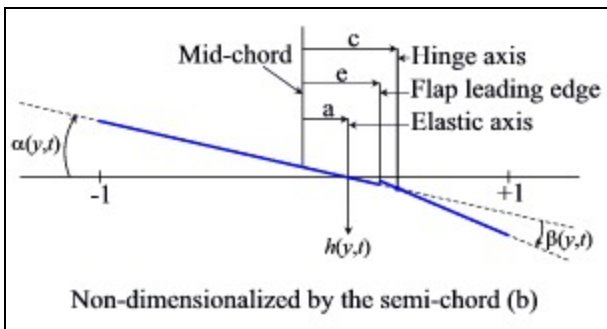


Fig. 1. Two-dimensional schematic of rotor blade with trailing-edge flap.

3 Development of Flutter Model

3.1 Normal Modes

The basic approach to the three-dimensional rotor blade flutter problem is similar to that developed by Scanlan and Rosenbaum [2] for a fixed-wing aircraft and Daughaday, DuWaldt, and Gates [16] for rotary-wing aircraft. Lagrange's equation is applied using the aerodynamic forces and moments given by two-dimensional strip theory for an incompressible flow, but with a modified lift deficiency function, such as Loewy's or a finite-wake model [17], [18]. The problem will be three-dimensional only to the extent that the blade sectional variations of mass, geometry and freestream velocity ($v = \Omega r$) are taken into account. It is assumed that the aerodynamic forces and moments do not change the uncoupled modes shapes.

The number of degrees of freedom that should consider depends on the particular design of the rotor blade and its corresponding structural properties. A hingeless rotor requires at least three degrees of freedom (3DOF) – the first blade bending mode (h_1), the first blade-torsional mode (α_1), and rigid-body motion for the trailing-edge flap (β_0). Scanlan and Rosenbaum [2] recommend that in general, if the frequency of the corresponding mode is less than 1.2 times that of the 1st blade torsional mode, then the mode shape should be considered. In most helicopter rotor blades the second and sometimes the third bending modes normally meet the conditions set by Scanlan and Rosenbaum.

Considering a 5DOF case for a hingeless rotor system incorporating a trailing-edge flap, the bending and torsional deflections can be written as

$$h(x,t) = h_1(t) f_1(x) + h_2(t) f_2(x) + h_3(t) f_3(x)$$

$$\alpha(x,t) = \alpha_1(t) F_1(x)$$

$$\beta(y,t) = \beta_0(t) G_0(y)$$

where it is assumed that the predominant motion of the trailing-edge flap is rigid-body motion (subscript 0). The terms containing the

displacement (y) are the characteristic functions (mode shapes) for the rotor blade, and the terms containing the time (t) are the normal coordinates that can be considered as weighting functions for each mode that contributes to the deflection. Since the rigid-body displacements of the trailing-edge flap are not set to a specific value, the displacements are eigenvectors that are relative to each other, and simple harmonic motion is assumed so that a flutter solution may be obtained. For rigid body trailing-edge flap motion, the free deflection motion can be written as

$$\omega_{\beta_0} = \sqrt{\frac{k_{\beta}}{I_{\beta}}}$$

where k_{β} is the torsional stiffness and I_{β} is the mass moment of inertia of the trailing-edge flap [1]. Since the torsional stiffness of the trailing-edge flap can be varied, it can be tuned such that the flap rigid body uncoupled natural frequency is equal to the flap input frequency. In this paper, the flap uncoupled natural frequencies will be restricted to integer multiples of the rotational velocity in order to study the effects of inputs corresponding to higher harmonic control and the natural filtering of frequencies provided by the rotor.

3.2 Application of Lagrange's Equation

Lagrange's equation is given as

$$\frac{d}{dt} \left(\frac{\partial T}{\partial \dot{q}_n} \right) - \frac{\partial T}{\partial q_n} + \frac{\partial U}{\partial q_n} + \frac{\partial D}{\partial \dot{q}_n} = Q_n$$

where $T \equiv$ kinetic energy, $U \equiv$ potential energy, $D \equiv$ dissipation function, and $Q_n \equiv$ generalized force. For the 5DOF case,

$$\begin{aligned} T &= \frac{1}{2} M_1 \dot{h}_1^2 + \frac{1}{2} M_2 \dot{h}_2^2 + \frac{1}{2} M_3 \dot{h}_3^2 + \frac{1}{2} I_{\alpha_1} \dot{\alpha}_1^2 \\ &\quad + \frac{1}{2} I_{\beta_0} \dot{\beta}_0^2 + S_{\alpha_1} \dot{h}_1 \dot{\alpha}_1 + S_{\alpha_2} \dot{h}_2 \dot{\alpha}_1 + S_{\alpha_3} \dot{h}_3 \dot{\alpha}_1 \\ &\quad + S_{\beta_0} \dot{h}_1 \dot{\beta}_0 + S_{\beta_2} \dot{h}_2 \dot{\beta}_0 + S_{\beta_3} \dot{h}_3 \dot{\beta}_0 + P_{\alpha_1 \beta_0} \dot{\alpha}_1 \dot{\beta}_0 \\ U &= \frac{1}{2} M_1 \omega_{h_1}^2 h_1^2 + \frac{1}{2} M_2 \omega_{h_2}^2 h_2^2 + \frac{1}{2} M_3 \omega_{h_3}^2 h_3^2 \\ &\quad + \frac{1}{2} I_{\alpha_1} \omega_{\alpha_1}^2 \alpha_1^2 + \frac{1}{2} I_{\beta_0} \omega_{\beta_0}^2 \beta_0^2 \end{aligned}$$

$$\begin{aligned} D &= \frac{M_1 g_{h_1} \omega_{h_1}^2 \dot{h}_1^2}{2\omega} + \frac{M_2 g_{h_2} \omega_{h_2}^2 \dot{h}_2^2}{2\omega} + \frac{M_3 g_{h_3} \omega_{h_3}^2 \dot{h}_3^2}{2\omega} \\ &\quad + \frac{I_{\alpha_1} g_{\alpha_1} \omega_{\alpha_1}^2 \dot{\alpha}_1^2}{2\omega} + \frac{I_{\beta_0} g_{\beta_0} \omega_{\beta_0}^2 \dot{\beta}_0^2}{2\omega} \end{aligned}$$

where M_n , I_{α_n} , and I_{β_n} are the generalized masses, S_{α_n} and S_{β_n} are the static imbalance terms, and $P_{\alpha_n \beta_n}$ are the mechanical coupling terms. The generalized forces are defined as

$$\begin{aligned} Q_{h_1} &= \pi \rho \omega^2 \left(A_{h_1 h_1} h_1 + A_{h_1 h_2} h_2 + A_{h_1 h_3} h_3 + A_{h_1 \alpha_1} \alpha_1 + A_{h_1 \beta_0} \beta_0 \right) \\ Q_{h_2} &= \pi \rho \omega^2 \left(A_{h_2 h_1} h_1 + A_{h_2 h_2} h_2 + A_{h_2 h_3} h_3 + A_{h_2 \alpha_1} \alpha_1 + A_{h_2 \beta_0} \beta_0 \right) \\ Q_{h_3} &= \pi \rho \omega^2 \left(A_{h_3 h_1} h_1 + A_{h_3 h_2} h_2 + A_{h_3 h_3} h_3 + A_{h_3 \alpha_1} \alpha_1 + A_{h_3 \beta_0} \beta_0 \right) \\ Q_{\alpha_1} &= \pi \rho \omega^2 \left(A_{\alpha_1 h_1} h_1 + A_{\alpha_1 h_2} h_2 + A_{\alpha_1 h_3} h_3 + A_{\alpha_1 \alpha_1} \alpha_1 + A_{\alpha_1 \beta_0} \beta_0 \right) \\ Q_{\beta_0} &= \pi \rho \omega^2 \left(A_{\beta_0 h_1} h_1 + A_{\beta_0 h_2} h_2 + A_{\beta_0 h_3} h_3 + A_{\beta_0 \alpha_1} \alpha_1 + A_{\beta_0 \beta_0} \beta_0 \right) \end{aligned}$$

and include the aerodynamic terms which couple the modes together and incorporate the unsteady force and moment equations defined by Ref. [15] and [18]. Assuming simple harmonic motion and applying Lagrange's equation to each of the five DOFs yields the matrix shown in Eq. (1).

3.2 Solving the Eigenvalue Problem

It can be seen that Eq. (1) is a set of complex homogenous equations where the primary variable is the flutter frequency (ω). Since it can be assumed that not all the displacements (h_1 , h_2 , h_3 , α_1 , and β_0) are simultaneously zero, the solution to the complex homogeneous equations is found by solving a complex eigenvalue problem of the form $(\bar{A} - IZ)X = 0$. Unfortunately, the blade structural damping coefficients in Eq. (1) are not easily obtained. To overcome this problem, Smilg and Wasserman [15] suggest a method that effectively equate the damping coefficients defined in the dissipation function, $g_{h_1} = g_{h_2} = g_{h_3} = g_{\alpha_1} = g_{\beta_0} = g$. By examining Eq. (1), it can be seen that the flutter frequency and the structural damping always appear together. Defining a complex variable

$$\begin{bmatrix}
 \left\{ \begin{array}{l} \pi\rho A_{h_1 h_1} + M_1 \\ -M_1 (1 + i g_{h_1}) \left(\frac{\omega_{h_1}}{\omega} \right)^2 \end{array} \right\} & \pi\rho A_{h_1 h_2} & \pi\rho A_{h_1 h_3} & \pi\rho A_{h_1 \alpha_1} + S_{\alpha_1} & \pi\rho A_{h_1 \beta_0} + S_{\beta_0} \\
 \pi\rho A_{h_2 h_1} & \left\{ \begin{array}{l} \pi\rho A_{h_2 h_2} + M_2 \\ -M_2 (1 + i g_{h_2}) \left(\frac{\omega_{h_2}}{\omega} \right)^2 \end{array} \right\} & \pi\rho A_{h_2 h_3} & \pi\rho A_{h_2 \alpha_1} + S_{\alpha_2} & \pi\rho A_{h_2 \beta_0} + S_{\beta_2} \\
 \pi\rho A_{h_3 h_1} & \pi\rho A_{h_3 h_2} & \left\{ \begin{array}{l} \pi\rho A_{h_3 h_3} + M_3 \\ -M_3 (1 + i g_{h_3}) \left(\frac{\omega_{h_3}}{\omega} \right)^2 \end{array} \right\} & \pi\rho A_{h_3 \alpha_1} + S_{\alpha_3} & \pi\rho A_{h_3 \beta_0} + S_{\beta_3} \\
 \pi\rho A_{\alpha_1 h_1} + S_{\alpha_1} & \pi\rho A_{\alpha_1 h_2} + S_{\alpha_2} & \pi\rho A_{\alpha_1 h_3} + S_{\alpha_3} & \left\{ \begin{array}{l} \pi\rho A_{\alpha_1 \alpha_1} + I_{\alpha_1} \\ -I_{\alpha_1} (1 + i g_{\alpha_1}) \left(\frac{\omega_{\alpha_1}}{\omega} \right)^2 \end{array} \right\} & \pi\rho A_{\alpha_1 \beta_0} + P_{\alpha_1 \beta_0} \\
 \pi\rho A_{\beta_0 h_1} + S_{\beta_0} & \pi\rho A_{\beta_0 h_2} + S_{\beta_2} & \pi\rho A_{\beta_0 h_3} + S_{\beta_3} & \pi\rho A_{\beta_0 \alpha_1} + P_{\alpha_1 \beta_0} & \left\{ \begin{array}{l} \pi\rho A_{\beta_0 \beta_0} + I_{\beta_0} \\ -I_{\beta_0} (1 + i g_{\beta_0}) \left(\frac{\omega_{\beta_0}}{\omega} \right)^2 \end{array} \right\}
 \end{bmatrix}
 \begin{bmatrix}
 h_1 \\
 h_2 \\
 h_3 \\
 \alpha_1 \\
 \beta_0
 \end{bmatrix} = 0$$

$$Z = \left(\frac{\omega_{\alpha_1}}{\omega} \right)^2 (1 + i g),$$

the solution to Eq. (1) can be written as

$$\begin{bmatrix}
 \bar{A}_{h_1 h_1} - Z & \bar{A}_{h_1 h_2} & \bar{A}_{h_1 h_3} & \bar{A}_{h_1 \alpha_1} & \bar{A}_{h_1 \beta_0} \\
 \bar{A}_{h_2 h_1} & \bar{A}_{h_2 h_2} - Z & \bar{A}_{h_2 h_3} & \bar{A}_{h_2 \alpha_1} & \bar{A}_{h_2 \beta_0} \\
 \bar{A}_{h_3 h_1} & \bar{A}_{h_3 h_2} & \bar{A}_{h_3 h_3} - Z & \bar{A}_{h_3 \alpha_1} & \bar{A}_{h_3 \beta_0} \\
 \bar{A}_{\alpha_1 h_1} & \bar{A}_{\alpha_1 h_2} & \bar{A}_{\alpha_1 h_3} & \bar{A}_{\alpha_1 \alpha_1} - Z & \bar{A}_{\alpha_1 \beta_0} \\
 \bar{A}_{\beta_0 h_1} & \bar{A}_{\beta_0 h_2} & \bar{A}_{\beta_0 h_3} & \bar{A}_{\beta_0 \alpha_1} & \bar{A}_{\beta_0 \beta_0} - Z
 \end{bmatrix} = 0$$

where the $A_{q_i q_j}$ are the aerodynamic terms which couple the modes and incorporate the unsteady force and moment equations defined by [15] and [18] using lumped parameter system:

Eq. (1). Rotor Blade Flutter Matrix

$$\begin{aligned}
 A_{h_1 h_1} &= \sum_{n=1}^N b_n^2 [f_1(y)]_n^2 (L_h)_n \\
 A_{h_1 h_2} &= \sum_{n=1}^N b_n^2 f_1(y)_n f_2(y)_n (L_h)_n \\
 A_{h_1 h_3} &= \sum_{n=1}^N b_n^2 f_1(y)_n f_3(y)_n (L_h)_n
 \end{aligned}$$

$$A_{h_1 \alpha_1} = \sum_{n=1}^N b_n^3 f_1(y)_n F_1(y)_n \left[(L_\alpha)_n - \left(\frac{1}{2} + a_n \right) (L_h)_n \right]$$

$$A_{h_1 \beta_0} = \sum_{n=n_1}^{n_2} b_n^3 f_1(y)_n G_0(y)_n \left[(L_\beta)_n - (c_n - e_n) (L_z)_n \right]$$

$$A_{h_2 h_1} = \sum_{n=1}^N b_n^2 f_2(y)_n f_1(y)_n (L_h)_n = A_{h_1 h_2}$$

$$A_{h_2 h_2} = \sum_{n=1}^N b_n^2 [f_2(y)]_n^2 (L_h)_n$$

$$A_{h_2 h_3} = \sum_{n=1}^N b_n^2 f_2(y)_n f_3(y)_n (L_h)_n$$

$$A_{h_2 \alpha_1} = \sum_{n=1}^N b_n^3 f_2(y)_n F_1(y)_n \left[(L_\alpha)_n - \left(\frac{1}{2} + a_n \right) (L_h)_n \right]$$

$$A_{h_2 \beta_0} = \sum_{n=n_1}^{n_2} b_n^3 f_2(y)_n G_0(y)_n \left[(L_\beta)_n - (c_n - e_n) (L_z)_n \right]$$

$$A_{h_3 h_1} = \sum_{n=1}^N b_n^2 f_3(y)_n f_1(y)_n (L_h)_n = A_{h_1 h_3}$$

$$A_{h_3 h_2} = \sum_{n=1}^N b_n^2 f_3(y)_n f_2(y)_n (L_h)_n = A_{h_2 h_3}$$

$$A_{h_3 h_3} = \sum_{n=1}^N b_n^2 [f_3(y)]_n^2 (L_h)_n$$

$$\begin{aligned}
 A_{h,\alpha_1} &= \sum_{n=1}^N b_n^3 f_3(y)_n F_1(y)_n \left[(L_\alpha)_n - \left(\frac{1}{2} + a_n \right) (L_h)_n \right] \\
 A_{h,\beta_0} &= \sum_{n=n_1}^{n_2} b_n^3 f_3(y)_n G_0(y)_n \left[(L_\beta)_n - (c_n - e_n) (L_z)_n \right] \\
 A_{\alpha,h_1} &= \sum_{n=1}^N b_n^3 F_1(y)_n f_1(y)_n \left[(M_h)_n - \left(\frac{1}{2} + a_n \right) (L_h)_n \right] \\
 A_{\alpha,h_2} &= \sum_{n=1}^N b_n^3 F_1(y)_n f_2(y)_n \left[(M_h)_n - \left(\frac{1}{2} + a_n \right) (L_h)_n \right] \\
 A_{\alpha,h_3} &= \sum_{n=1}^N b_n^3 F_1(y)_n f_3(y)_n \left[(M_h)_n - \left(\frac{1}{2} + a_n \right) (L_h)_n \right] \\
 A_{\alpha,\alpha_1} &= \sum_{n=1}^N b_n^4 [F_1(y)]_n^2 [(M_\alpha)_n \\
 &\quad - \left(\frac{1}{2} + a_n \right) ((L_\alpha)_n + (M_h)_n) + \left(\frac{1}{2} + a_n \right)^2 (L_h)_n] \\
 A_{\alpha,\beta_0} &= \sum_{n=n_1}^{n_2} b_n^4 F_1(y)_n G_0(y)_n \left[(M_\beta)_n - \left(\frac{1}{2} + a_n \right) (L_\beta)_n \right. \\
 &\quad \left. - (c_n - e_n) (M_z)_n + (c_n - e_n) \left(\frac{1}{2} + a_n \right) (L_z)_n \right] \\
 A_{\beta,h_1} &= \sum_{n=n_1}^{n_2} b_n^3 G_0(y)_n f_1(y)_n [(T_h)_n - (c_n - e_n) (P_h)_n] \\
 A_{\beta,h_2} &= \sum_{n=n_1}^{n_2} b_n^3 G_0(y)_n f_2(y)_n [(T_h)_n - (c_n - e_n) (P_h)_n] \\
 A_{\beta,h_3} &= \sum_{n=n_1}^{n_2} b_n^3 G_0(y)_n f_3(y)_n [(T_h)_n - (c_n - e_n) (P_h)_n] \\
 A_{\beta,\alpha_1} &= \sum_{n=n_1}^{n_2} b_n^4 G_0(y)_n F_1(y)_n [(T_\alpha)_n \\
 &\quad - (c_n - e_n) (P_\alpha)_n + \left(\frac{1}{2} + a_n \right) (T_h)_n \\
 &\quad + \left(\frac{1}{2} + a_n \right) (c_n - e_n) (P_h)_n] \\
 A_{\beta_0\beta_0} &= \sum_{n=n_1}^{n_2} b_n^4 [G_0(y)]_n^2 [(T_\beta)_n - (c_n - e_n) ((P_\beta)_n + (T_z)_n) \\
 &\quad + (c_n - e_n)^2 (P_z)_n]
 \end{aligned}$$

The definition of Z is somewhat arbitrary, but it is a complex quantity that has a ratio of a reference frequency to the flutter frequency in its real part and a product of the flutter frequency and the damping coefficient in the imaginary part. Since the first torsional frequency is used as the reference frequency for

determining whether or not to include a mode, it becomes the most logical choice as the reference frequency for Z .

4 Flutter Analysis Using Example Rotor Blade

Due to the proprietary rights of many of the current rotor blades under development, it became necessary to develop an example rotor blade that could be used in the analysis to demonstrate the robustness and applicability of the theory. The example rotor blade chosen is a hingeless design that is similar to the rotor blade described in Table B-17 of TRECOM Technical Report 64-15 [19], which is modelled after the blade designed for the Sikorsky H-3 (S-61). This rotor blade has a length of 31 feet ($R = 31$ ft.) and is part of a five-bladed helicopter ($N_b = 5$) with a gross weight of 16,800 lbs. The primary differences between the TRECOM blade and the example blade is that a 25% chord, trailing-edge flap has been incorporated from station 279 to 334 on the rotor blade, the root end restraint has been modified from an articulated design to a hingeless design, and the mass of the blade has been redistributed to account for added weight of the flap but designed in such a manner that the overall mass of the blade remains the same. Additionally, the c.g. of the rotor blade where the flap has been incorporated has been shifted from 25% chord to 40% chord to show effects of c.g. displacement on the flutter speed.

Figures 2 through 7 are plots of natural frequency and damping coefficient required for flutter to exist versus a non-dimensionalized rotational velocity for different choices of lift deficiency function (Theodorsen or Loewy) and different values of flap stiffness, k_β , in which $\omega_{\beta_0} = \sqrt{k_\beta / I_{\beta_0}}$. Note that a negative value of g is the stable condition since damping must be reduced to cause flutter to exist. The flutter speed is determined by noting the velocity at which the damping coefficient is zero. It can be shown that layers of shed vorticity beneath the rotor have a significant effect on aerodynamic coefficients [18]. When comparing Loewy's lift

deficiency function with an infinite number of previously shed wakes to the finite wake lift deficiency function with just a single previously shed wake, it can be seen that the number of wakes has a lesser effect than frequency ratio, which effectively is the phase relationship between the shed layers of vorticity. Thus, frequency ratio will also have a significant effect on the flutter solution due to the larger changes to aerodynamic coefficients caused by changes in frequency ratio. The case of $m = 0$ (wakes completely in phase) always yielded the highest flutter speed, and the case of $m = 0.25$ yielded the lowest flutter speed. The reason for this phenomenon can be seen in Fig. 8 from Loewy [10] in which the pitch damping coefficient, defined by

$$C_{pitch-damping} = \frac{1}{k} \left[\left(\frac{1}{2} - a \right) - \left(\frac{1}{2} + a \right) \frac{2G'}{k} - \left(\frac{1}{4} - a^2 \right) 2F' \right],$$

is plotted against the frequency ratio for various wake spacings (inflow parameter). It can be seen that the pitch damping coefficient becomes negative (unstable) in the region where $m = 1.25$. The wake weighting function is periodic in m , and the $m = 0.25$ case shown in Fig. 8 could correspond to any integer plus 0.25 case. Thus, this decreased pitch damping has a destabilizing effect on the flutter speed of the rotor blade.

This destabilizing effect was also noted by Jones and Platzer [20] and Turner [21]. Jones and Platzer used a panel code to plot the time rate change of the pitch amplitude against frequency ratio for the case of a single wake beneath an airfoil that was oscillating in pure pitch about the leading edge ($a = -1.0$). Their results showed an instability for $1.52 \leq m \leq 1.84$, which is consistent with Figure 16 ($a = -1.0$) from Loewy. Since the example rotor blade had an aft c.g. offset in the sections with trailing-edge flaps, the effect on pitch damping would be similar to moving the elastic axis aft towards the midchord.

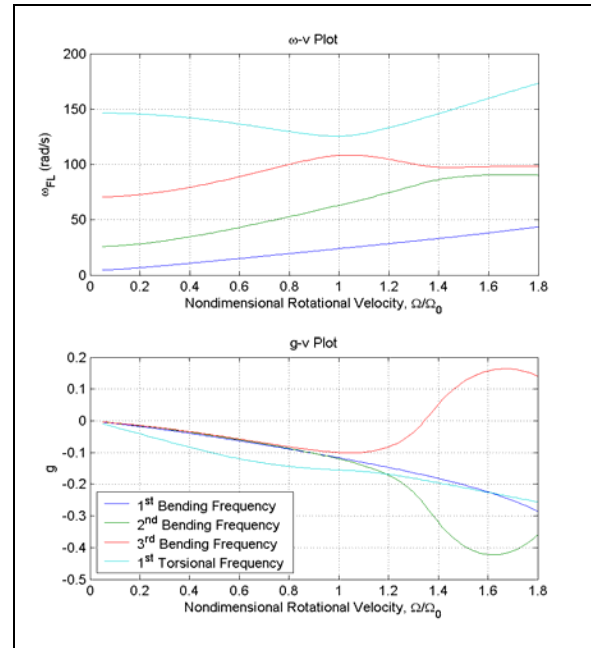


Fig. 2. g - Ω plot for example rotor blade using Theodorsen's lift deficiency function ($\omega_\beta = 0P$).

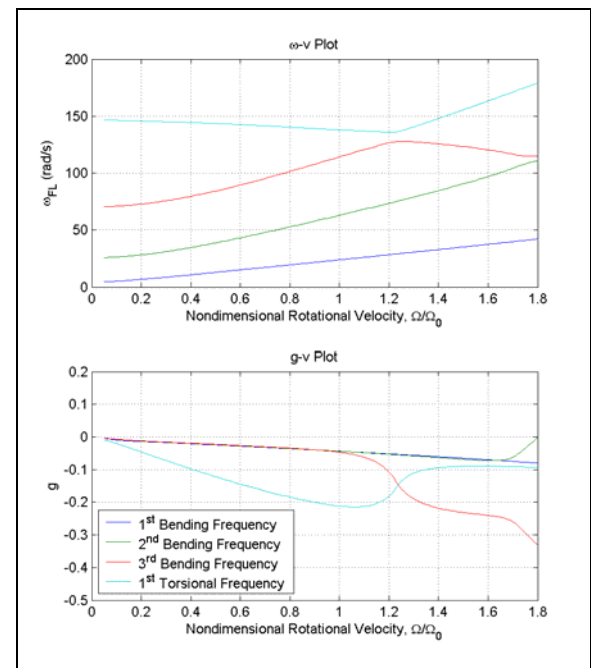


Fig. 3. g - Ω plot for example rotor blade using Loewy's lift deficiency function, $m = 0$ ($\omega_\beta = 0P$).

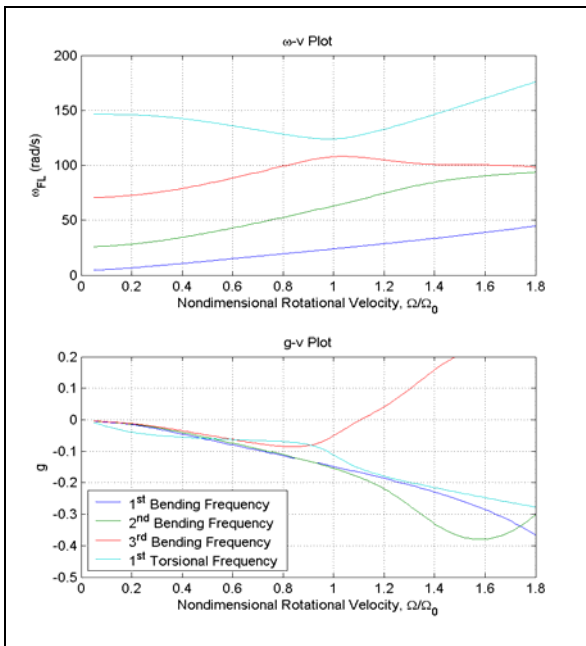


Fig. 4. g - Ω plot for example rotor blade using Loewy's lift deficiency function, $m = 0.25$ ($\omega_\beta = 0P$).

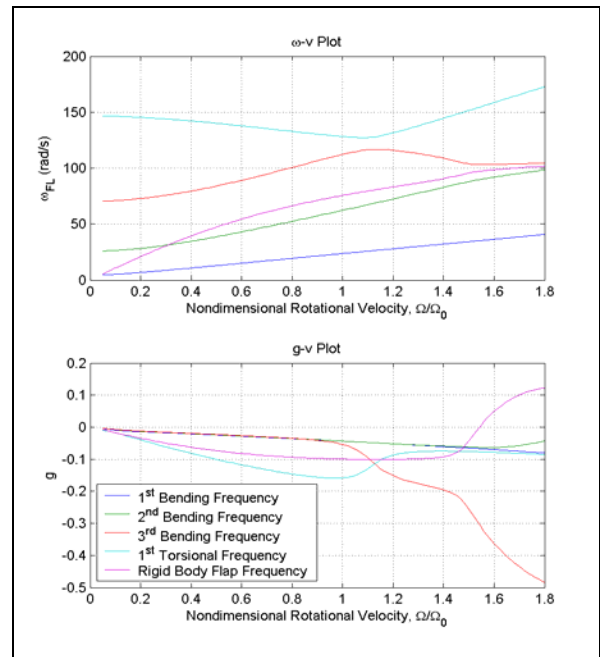


Fig. 6. g - Ω plot for example rotor blade using Loewy's lift deficiency function, $m = 0$ ($\omega_\beta = 5P$).

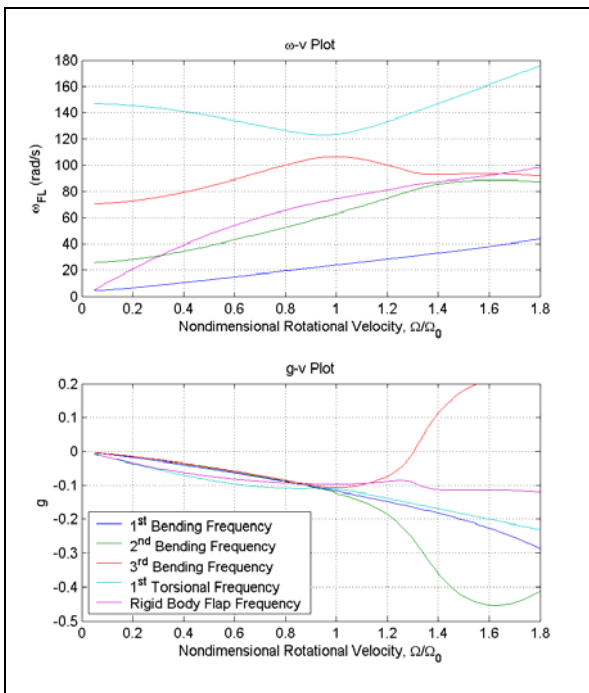


Fig. 5. g - Ω plot for example rotor blade using Theodorsen's lift deficiency function ($\omega_\beta = 5P$).

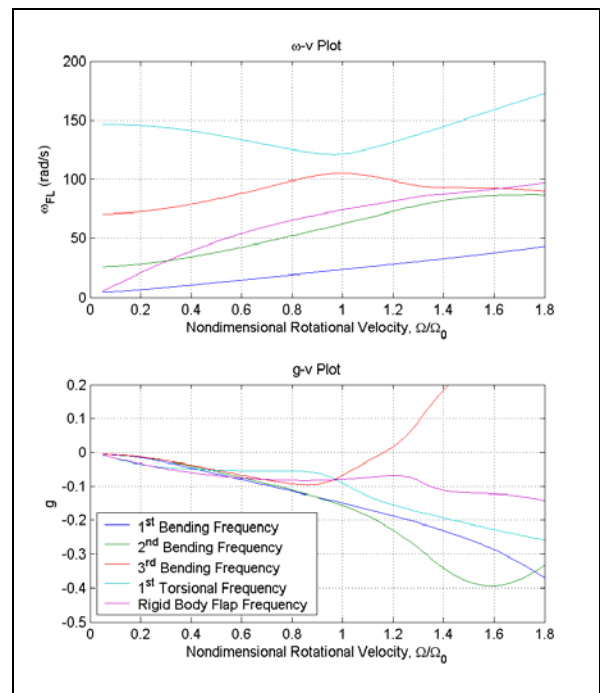


Fig. 7. g - Ω plot for example rotor blade using Loewy's lift deficiency function, $m = 0.25$ ($\omega_\beta = 5P$).

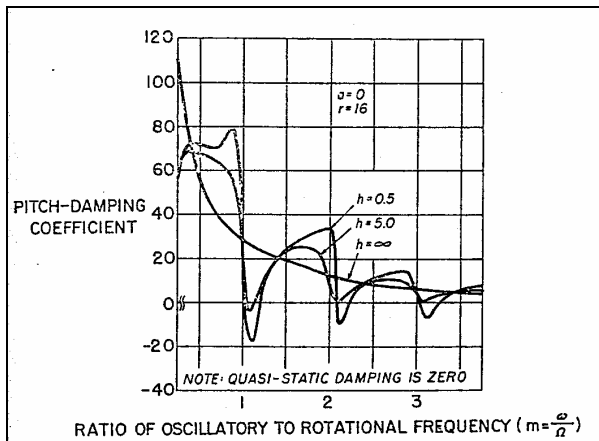


Fig. 8. Pitch damping coefficient versus frequency ratio ($a = 0$) (from [10]).

5 Conclusion

The solution to the flutter problem for rotary-wing aircraft is inherently more complicated than its fixed-wing counterpart, especially for rotor blades with trailing-edge flaps. The frequency-domain approach is used here to develop the flutter equations of motion that could be used quickly and easily without the need to learn all the ins and outs of one of the rotor dynamics computational codes. The method may be easily programmed in any language that has access to an eigenvalue subroutine that can handle complex coefficients. It was seen that the frequency ratio (m), which effectively measures the phase relationship between shed layers of vorticity, was the lift deficiency function parameter that affected the results the most with a destabilizing effect seen near $m = 0.25$.

References

[1] Bisplinghoff, R. L., Ashley, H., and Halfman, R. L., *Aeroelasticity*, Addison-Wesley Publishing Company, Inc., Cambridge, Massachusetts, 1955.

[2] Scanlan, R. H. and Rosenbaum, R., *Introduction to the Study of Aircraft Vibration and Flutter*, The MacMillan Company, New York, 1951.

[3] "Certification of Normal Category Rotorcraft," Federal Aviation Administration Aircraft Circular 27-1B, September 30, 1999.

[4] "Certification of Transport Category Rotorcraft," Federal Aviation Administration Aircraft Circular 29-2C, September 30, 1999.

[5] Straub, F. K. and Charles, B. D., "Comprehensive Modeling of Rotor Blades with Trailing Edge Flaps," Proceedings of the 55th Annual Form of the American Helicopter Society, Montreal, Quebec, Canada, May 1999.

[6] Wood, E. R., Couch, M. A., and Canright, D., "On the Flutter Speed of a Rotor Blade in Forward Flight," 28th European Rotorcraft Forum, Bristol, England, 17-20 September 2002.

[7] Johnson, W., "Rotorcraft Dynamics Models for a Comprehensive Analysis." Proceedings of the 54th Annual Forum of the American Helicopter Society, Washington, D.C., May 1998.

[8] Milgram, J., Chopra, I., and Straub, F., "A Comprehensive Rotorcraft Aeroelastic Analysis with Trailing Edge Flap Model: Validation with Experimental Data," Proceedings of the 52nd Annual Forum of the American Helicopter Society, Washington, D.C., June 1996.

[9] Couch, M. A. and Wood, E. R., "A 2-D Unsteady Aerodynamic Application to HHC Test Data Show Performance Improvements," AIAA paper 2002-6017 to be presented at 2002 Biennial International Powered Lift Conference and Exhibit, Williamsburg, Virginia, 5-7 November 2002.

[10] Loewy, R. G., "A Two-Dimensional Approach to the Unsteady Aerodynamics of Rotary Wings," *Journal of the Aeronautical Sciences*, Vol. 24, No. 2, pp. 81-92, February 1957.

[11] Theodorsen, T., "General Theory of Aerodynamic Instability and the Mechanism of Flutter," NACA Technical Report No. 496, 1935.

[12] Den Hartog, J. P., *Mechanical Vibrations*, Dover Publications, New York, 1985.

[13] Myklestad, N. O., "A New Method of Calculating Natural Modes of Uncoupled Bending Vibrations of Airplane Wings and Other Types of Beams," *Journal of the Aeronautical Sciences*, Vol. 11, No. 4, April 1944, pp. 153-162.

[14] Gerstenberger, W. and Wood, E. R., "Analysis of Helicopter Aeroelastic Characteristics in High-Speed Flight," *AIAA Journal*, Vol. 1, No. 10, October 1963.

[15] Smilg, B. and Wasserman, L. S., "Application of Three-Dimensional Flutter Theory to Aircraft Structures (With Corrections for the Effects of Control Surface Aerodynamic Balance and Geared Tabs)," *Army Air Corps Technical Report (AAFTR) 4798*, Dayton, Ohio, July 1942.

- [16] Daughaday, H., DuWaldt, F., and Gates, C., "Investigation of Helicopter Blade Flutter and Load Amplification Problems," *Journal of the American Helicopter Society*, Vol. 2, No. 3, pp. 27-45, July 1957.
- [17] Couch, M. A., "A Finite Wake Theory for Two-Dimensional Rotary Wing Unsteady Aerodynamics," Master's Thesis, Naval Postgraduate School, September 1993.
- [18] Couch, M. A. "A Three-Dimensional Flutter Theory for Rotor Blades with Trailing-Edge Flaps," Ph.D. Dissertation, Naval Postgraduate School, June 2003.
- [19] Wood, E. R. and Buffalano, A. C., "Parametric Investigation of the Aerodynamic and Aeroelastic Characteristics of Articulated and Rigid (Hingeless) Helicopter Rotor Systems," TRECOM Technical Report 64-15, April 1964.
- [20] Jones, K. D. and Platzer, M. F., "Time-Domain Analysis of Low-Speed Airfoil Flutter," *AIAA Journal*, Vol. 34, No. 5, pp.1027-1033.
- [21] Turner, M. A., "A Computational Investigation of Wake-Induced Airfoil Flutter in Incompressible Flow and Active Flutter Control," Master's Thesis, Naval Postgraduate School, March 1994.